

# Tungsten oxide nanowire growth by chemically-induced strain

Christian Klinke,\* James B. Hannon, Lynne Gignac, Kathleen Reuter, and Phaedon Avouris  
IBM T. J. Watson Research Center, 1101 Kitchawan Road, Yorktown Heights, NY 10598, USA

We have investigated the formation of tungsten oxide nanowires under different CVD conditions. We find that exposure of oxidized tungsten films to hydrogen and methane at 900°C leads to the formation of a dense array of typically 10 nm diameter nanowires. Structural and chemical analysis shows that the wires are crystalline  $\text{WO}_3$ . We propose a chemically-driven whisker growth mechanism in which interfacial strain associated with the formation of tungsten carbide stimulates nanowire growth. This might be a general concept, applicable also in other nanowire systems.

Interest in semiconducting nanowires continues to grow, in part, because of their potential in nanoelectronics and optoelectronics [1]. To date, a wide variety of nanowire-based devices have been demonstrated, including photodetectors, photodiodes, and sensors [2]. Nanowires offer certain advantages over planar devices. For example, strain arising from lattice mismatch can be accommodated via radial relaxation, rather than through the creation of bulk dislocations, allowing new types of heterojunctions to be formed [3]. The high surface/volume ratio can also make nanowires efficient sensors [4].

The majority of nanowires are grown using the vapor-liquid-solid (VLS) mechanism, in which the nanowire grows from a small, liquified gold catalyst particle [5, 6]. The size of the catalyst particle determines the diameter of the nanowire. Tungsten oxide nanowires, on the other hand, grow by a completely different mechanism that does not involve catalyst particles. Several groups have shown that oxide whiskers can form when tungsten substrates are heated in various mixtures of argon, hydrogen, and oxygen [7, 8, 9, 10]. While it is clear that the growth mechanism is not related to VLS, it is unclear how and why the nanowires form. We have grown tungsten oxide nanowires with a high-yield process that gives new insight into the driving forces for nanowire formation. We find that exposure of oxidized tungsten surfaces to first hydrogen and then methane increases the yield of the nanowires by about two orders of magnitude compared to a process that involves hydrogen, methane, or argon alone. Chemical characterization shows that the wires are crystalline  $\text{WO}_3$  and that WC has formed on the substrate. We propose that the formation of tungsten carbide at the surface strains the surface oxide leading to enhanced whisker growth following a mechanism described by Fisher *et al.* [11] and Franks [12] in the 1950s. Our results show for the first time that nanowire growth can be significantly enhanced by chemically induced strain, in this case through the formation of tungsten carbide at the substrate.

Tungsten oxide has received considerable attention due to its application as a sensor material. Its bandgap lies in the optical spectrum, making it attractive for optics ap-

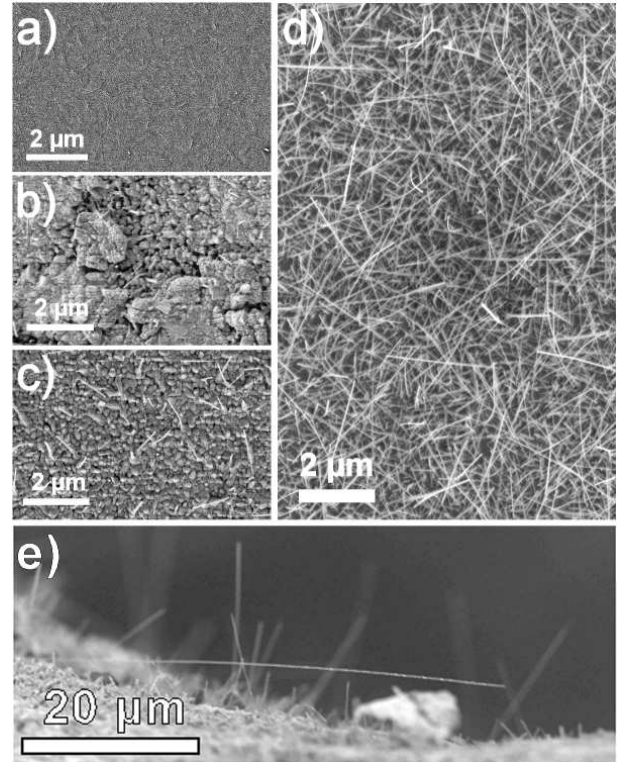


FIG. 1: SEM micrographs of a) the pristine tungsten substrate, and nanowires grown at 900°C with b) Ar, c) Ar +  $\text{H}_2$ , and d)  $\text{CH}_4 + \text{H}_2$  in the CVD system. e) The nanowires can be up to 40 μm long.

plications. Tungsten oxide has also been widely studied due to its ‘chromogenic’ properties [13]. That is, the optical properties can be varied by exposure to heat, light, or an applied potential. The same properties make tungsten oxide a promising material in applications ranging from sensors [14], to “smart windows” [15].

We used two different CVD systems to investigate nanowire growth. In the first, a standard 10 cm diameter tube furnace was used. The substrates – either tungsten wires, foils, or evaporated thin films (100 nm tungsten on silicon) – were introduced into the furnace on a quartz holder. The furnace was evacuated to a base pressure of 1 Torr. Our three-step process involved a heating phase followed by a growth phase, and then slow cooling to

\*Electronic address: klinke@chemie.uni-hamburg.de

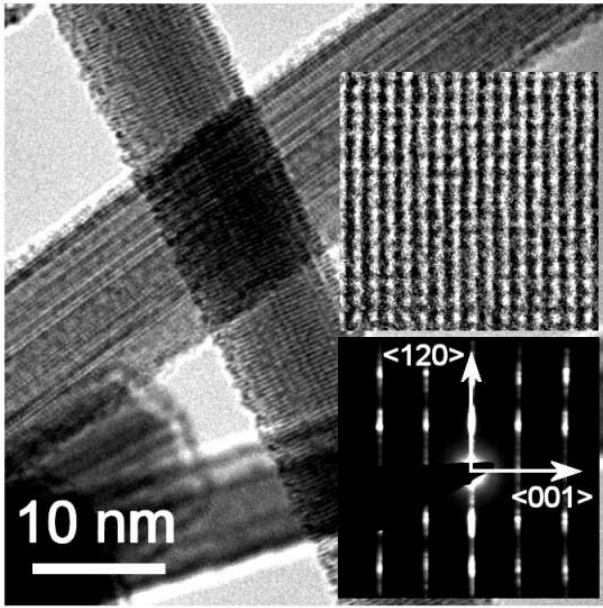


FIG. 2: TEM micrographs showing the lattice fringes and the diffraction pattern (insets) of individual tungsten oxide nanowires. The long axis of the wires points in  $\langle 001 \rangle$  direction of  $\text{WO}_3$ .

room temperature. In the heating phase, the temperature is ramped to  $900^\circ\text{C}$  at a rate of  $50^\circ/\text{min}$  in a gas flow of 500 sccm Ar and 200 sccm  $\text{H}_2$  (total pressure of 100 Torr). In the growth phase the temperature is held at  $900^\circ\text{C}$  in a mixture of 200 sccm hydrogen and 500 sccm methane for 30 min at a pressure of 100 Torr. Finally, the samples were cooled to room temperature in a gas flow of 500 sccm Ar.

In the first experiments, nanowires were grown by heating W films (Fig. 1a) in an Ar flow in the tube furnace. A scanning electron microscopy (SEM) image of a film exposed to 500 sccm Ar at  $900^\circ\text{C}$  is shown in Fig. 1b. Under these growth conditions the film partially dewets and roughens. The surface features are rounded and smooth (i.e. no facets), and very few nanowires are observed. However, we found that by adding  $\text{H}_2$  to the gas flow (e.g. 500 sccm Ar + 200 sccm  $\text{H}_2$ ), we obtained a more uniform surface consisting of crystallites that were clearly faceted (Fig. 1c), while the nanowire yield remained relatively low. A dramatic change in the growth occurs when the growth stage flow includes methane (Fig. 1d). The yield of nanowires for the mixed flow is about two orders of magnitude higher than when either hydrogen or methane are used separately. The nanowires are often several microns long, with a typical diameter of about 10 nm. Occasionally, we observed extremely long nanowires of up to  $40\text{ }\mu\text{m}$  in length (Fig. 1e).

We systematically varied the process conditions to investigate the influence of temperature, gas pressure, growth time, and gas mixture on the yield and length of the nanowires. We found that nanowires grew in the tem-

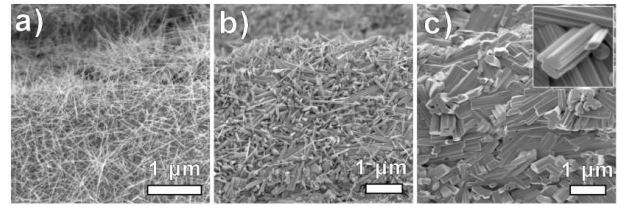


FIG. 3: Evolution of the morphology of the tungsten oxide nanowire film grown in the vacuum system with increasing temperature (from left to right). The comparison of pyrometric measurements along the heated filament with the corresponding SEM images allows to estimate the temperature in this series to be between  $800$  and  $950^\circ\text{C}$ .

perature range from  $600^\circ\text{C}$  to  $1000^\circ\text{C}$ . However, only at  $900^\circ\text{C}$  did we observe a high yield, with wires longer than  $1\text{ }\mu\text{m}$ . Above  $900^\circ\text{C}$  tungsten oxide starts to sublime in vacuum [13]. Surprisingly, extending the duration of the growth phase did not increase either the areal density or length of the wires. Furthermore, the yield was essentially unchanged when the total pressure of the growth phase mixture was varied from 10 to 500 Torr. Varying the methane/hydrogen ratio over a wide range also had no significant influence on the wire length or diameter. To summarize, high yield requires hydrogen pretreatment followed by exposure to methane.

In order to determine the chemical composition and structure of individual nanowires we grew them directly on transmission electron microscopy (TEM) grids made of tungsten. TEM images show that the wires are crystalline, with fringes visible both perpendicular and parallel to the wire axis (Fig. 2). The corresponding lattice distances are  $3.3\text{ }\text{\AA}$  and  $3.7\text{ }\text{\AA}$ , consistent with the structure of  $\text{WO}_3$ . The corresponding diffraction image (Fig. 2 inset) suggests that the wires are monoclinic  $\text{WO}_3$ , with the  $\langle 001 \rangle$  crystal axis oriented parallel to the long axis of the wire. The streaking in the direction orthogonal to the long axis indicates significant twinning. Energy dispersive X-ray (EDX) measurements and electron energy loss spectroscopy (EELS) performed directly on individual nanowires confirmed the presence of only tungsten and oxygen in the wires. X-ray photoelectron spectroscopy (XPS) was used to investigate the chemical composition of the nanowires and substrates after growth. The chemical shifts of the W 4f levels are compatible with a mixture of WC and  $\text{WO}_3$ . Samples measured before growth show no carbide peak. As we describe below, tungsten carbide is formed on the W substrate during the exposure to methane.

In order to determine the source of the oxygen in the nanowires, we grew them in a vacuum system with a base pressure of about  $10^{-7}$  Torr. The substrates consisted of resistively-heated W filaments. Nanowires were grown by first backfilling the chamber to 200 mTorr with  $\text{H}_2$ . The filament was then heated for 30 min at  $1000^\circ\text{C}$  (at the hottest point of the wire). Subsequently, the cham-

ber was pumped to  $10^{-7}$  Torr again and  $\text{CH}_4$  was introduced until the pressure reached 5 Torr. The filament was heated for 30 min in the methane atmosphere, and then cooled to room temperature. This process resulted in nanowire growth that was qualitatively similar to that achieved in the tube furnace: a high density of nanowires with a typical diameter of about 10 nm (Fig. 3a). However, if the filament was flashed to  $2000^\circ\text{C}$  just prior to processing, no nanowires were observed. We propose that the oxygen required for nanowire formation comes from the native oxide on the W substrates. The fact that the nanowire length can not be extended by extending the growth time supports this conclusion.

In the vacuum system the filament was clamped to thick Cu feedthroughs, resulting in a significant temperature gradient along the length of filament. The gradient allowed us to systematically investigate the role of temperature on the nanowire growth under otherwise identical process conditions. A sequence of SEM images along the filament length (i.e. with increasing temperature) is shown in Fig. 3. As the temperature is increased, the density and length of the nanowires *decreases*, while their diameter *increases*. As we describe below, this behavior is consistent with conventional whisker growth. Whiskers are non-equilibrium structures that grow as a result of bulk dislocation motion (i.e. climb). In one scenario described by Frank [16], the intersection of a dislocation with the surface traces out a periodic loop. Each time the loop is traversed, the area of the surface enclosed by the loop will be displaced by a Burger's vector. This mechanism gives rise to whiskers with irregular cross-sections but smooth side walls, as shown in in Fig. 3c(inset). The shape cross section is determined by the loop that the dislocation core traces at the surface (the path is ultimately determined by irregularities in surface morphology). Whisker growth is thought to be governed by bulk vacancy motion (in this case, presumably the tungsten oxide given the low mobility of vacancies in W at  $1000^\circ\text{C}$ ). In simple geometries [16], the whisker growth rate is (approximately) proportional to the the inverse of the wire diameter. It is clear from the data shown in Fig. 3 that nanowires with larger diameters are shorter than those with smaller diameters, consistent with that prediction. We conclude that the nanowires grow via dislocation climb in the oxide film.

While the growth *mechanism* is consistent with whisker growth, the driving force for whisker formation is less clear. In many metal whisker systems (e.g. Sn) the oxidation of the whisker surface plays an important role in stabilizing the growth of elongated structures with large surface area to volume ratios. In the present case the surface is already oxidized and the amount of oxide appears to be conserved. One possible driving force for whisker growth in the present case is interfacial strain: whisker growth will convert strained oxide at the W/ $\text{WO}_3$  interface to unstrained oxide in the nanowire. The relief of strain may be one important factor driving whisker formation.

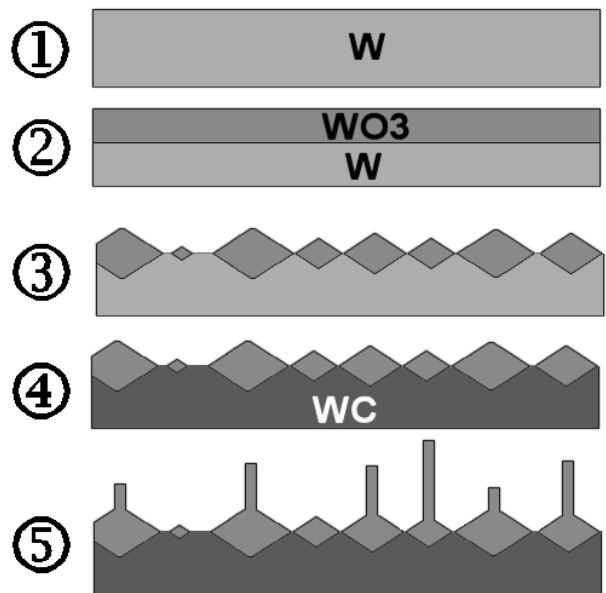


FIG. 4: *Proposed growth mechanism: The tungsten substrate (1) gets oxidized in air (2). In the CVD system at elevated temperatures the tungsten oxide surface roughens and forms sharp faceted crystallites with the help of hydrogen (3). Introduced  $\text{CH}_4$  carburizes the underlying tungsten. Carbide formation in turn induces strain at the WC/ $\text{WO}_3$  interface (4). The strain is relieved by formation of stress-free nanowires (5).*

We propose that the strain driving the whisker formation is enhanced by carbide formation at the W/ $\text{WO}_3$  interface. In this picture carbide formation increases the interfacial strain (e.g. the W-W separation in WC increases by %4), enhancing nanowire growth. A similar enhancement has been observed in Sn films subjected to external loading [11, 12]. The difference is that in the present case the strain is induced *chemically*, via carbide formation at the interface. The process is illustrated schematically in Fig. 4.

In order to clarify the role of the carbide at the interface, we attempted to re-grow nanowires on the same substrate. That is, we first grew nanowires in the vacuum system on a pristine filament using the procedure outlined above. The filament was then sonicated to remove the nanowires, and left in air for several days. It was then reintroduced into the vacuum system and subjected to the nanowire growth process for a second time. However, no nanowires grew during the second processing. The filament was irreversibly changed in the first processing, presumably because the carbide we measure using XPS is formed at the surface. Note that TEM measurements show no evidence for carbide formation in the nanowires. Subsequent processing does not produce nanowires because either, (a) no oxide forms on the carbide surface, or (b) further carbide formation does not change the strain state of the native oxide. We conclude

that carbide formation at the W/WO<sub>3</sub> *interface* is associated with the high nanowire yield. Hydrogen pretreatment is also required for high yield. As the Fig. 1c shows, hydrogen pretreatment significantly changes the surface morphology, presumably by enhancing oxide diffusion. H<sub>2</sub> is known to enhance oxygen diffusion in semiconductors [17]. In whisker growth, the whisker diameter is determined by surface morphology. Hydrogen pretreatment may help in forming the crystalline grains required for classical whisker growth.

In conclusion, our results show that exposure to both hydrogen and methane strongly enhances the formation of nanowires on (natively) oxidized W films during CVD processing. Structural and chemical analysis indicates

that the nanowires are crystalline WO<sub>3</sub> and that WC is formed at the surface of the tungsten substrates. The cross sectional shape and variation in nanowire length with diameter are consistent with conventional whisker growth. We conclude that interfacial strain drives the nanowire formation in a process analogous to that observed in mechanically strained Sn films. This wire growth mechanism is expected to be general, and may be of use in enhancing the yield in other nanowire systems.

We thank Bruce Ek for technical support. Christian Klinke acknowledges financial support from the Alexander-von-Humboldt Foundation.

- 
- [1] Wang, Z. L. *Adv. Mater.* **2003**, *15*, 432.
  - [2] Vayssieres, L. *Adv. Mater.* **2003**, *15*, 464.
  - [3] Björk, M. T.; Ohlsson, B. J.; Sass, T.; Persson, A. I.; Thelander, C.; Magnusson, M. H.; Deppert, K.; Wallenberg, L. R.; Samuelson, L. *Appl. Phys. Lett.* **2002**, *80*, 1058.
  - [4] Wan, Q.; Li, Q. H.; Chen, Y. J.; Wang, T. H.; He, X. L.; Li, J. P.; Lin, C. L. *Appl. Phys. Lett.* **2004**, *84*, 3654.
  - [5] Whisker Technology, ed. A.P. Levitt, Wiley-Interscience, New York, 1970.
  - [6] Law, M.; Goldberger, J.; Yang, P. *Annu. Rev. Mat. Res.* **2004**, *34*, 83.
  - [7] Okuyama, M. *Japan. J. Appl. Phys.* **1970**, *9*, 409.
  - [8] Gu, G.; Zheng, B.; Han, W. Q.; Roth, S.; Liu, J. *Nano Lett.* **2002**, *2*, 849.
  - [9] Li, X. L.; Liu, J. F.; Li, Y. D. *Inorg. Chem.* **2003**, *42*, 921.
  - [10] Zhang, H.; Feng, M.; Liu, F.; Liu, L.; Chen, H.; Gao, H.; Li, J. *Chem. Phys. Lett.* **2004**, *389*, 337.
  - [11] Fisher, R. M.; Darken, L. S.; Carroll, K. G. *Acta Metall.* **1954**, *2*, 368.
  - [12] Franks, J. *Acta Metall.* **1958**, *6*, 103.
  - [13] Bange, K. *Sol. Energy Mater. Sol. Cells* **1999**, *58*, 1.
  - [14] Cantalini, C.; Sun, H. T.; Faccio, M.; Pelino, M.; Santucci, S.; Lozzi, L.; Passacantando, M. *Sens. Actu. B* **1996**, *31*, 81.
  - [15] Cui, H. N.; Costa, M. F.; Teixeira, V.; Porqueras, I.; Bertran, E. *Surf. Sci.* **2003**, *532*, 1127.
  - [16] Frank, F. C. *Philos. Mag.* **1953**, *44*, 854.
  - [17] Jones, R. *Phil. Trans. Roy. Soc. A* **1995**, *350*, 189.